Relationship between structure and biochemical phenotype of lecithin:cholesterol acyltransferase (LCAT) mutants causing fish-eye disease

Berlinda Vanloo,* Frank Peelman,* Kristof Deschuymere,* Josee Taveirne,* Annick Verhee,† Catherine Gouyette,§ Christine Labeur,* Joël Vandekerckhove,† Jan Tavernier,† and Maryvonne Rosseneu[1,*]

Laboratory for Lipoprotein Chemistry,* and the Flanders Interuniversity Institute for Biotechnology,† Department of Medical Protein Research, Faculty of Medicine, Department of Biochemistry, University of Gent, B-9000 Gent, Belgium, and Unite Chimie Organique,§ Institut Pasteur, Paris, France

Abstract **In order to test the hypothesis that fish-eye disease (FED) is due to a deficient activation of lecithin:cholesterol acyltransferase (LCAT) by its co-factor apolipoprotein (apo) A-I, we overexpressed the natural mutants T123I, N131D, N391S, and other engineered mutants in Cos-1 cells. Esterase activity was measured on a monomeric phospholipid enelogue, phospholipase A_2 activity was measured on reconstituted high density lipoprotein (HDL), and acyltransferase activity was measured both on rHDL and on low density lipoprotein (LDL). The natural FED mutants have decreased phospholipase A_2 activity on rHDL, which accounts for the decreased acyltransferase activity previously reported. All mutants engineered at positions 131 and 391 had decreased esterase activity on a monomeric substrate and decreased acyltransferase activity on LDL. In contrast, mutations at position 123 preserved these activities and specifically decreased phospholipase A_2 and acyltransferase activites on rHDL. Mutations of hydrophilic residues in amphipathic helices α 3–4 and α His to an alanine did not affect the mutants' activity on rHDL. Based upon the 3D model built for human LCAT, we designed a new mutant F382A, which had a biochemical phenotype similar to the natural T123I FED mutant. These data suggest that residues T123 and F382, located N-terminal of helices α 3–4 and α His, contribute specifically to the interaction of LCAT with HDL and possibly with its co-factor apoA-I. Residues N131 and N391 seem critical for the optimal orientation of the two amphipathic helices necessary for the recognition of a lipoprotein substrate by the enzyme.**—Vanloo, B., F. Peelman, K. Deschuymere, J. Taveirne, A. Verhee, C. Gouyette, C. Labeur, J. Vandekerckhove, J. Tavernier, and M. Rosseneu. **Relationship between structure and biochemical phenotype of lecithin:cholesterol acyltransferase (LCAT) mutants causing fish-eye disease.** ***J. Lipid Res.*** **2000.** 41: **752–761.**

Supplementary key words cholesterol • phospholipid • enzyme • lipase • HDL • LDL • esterase • acyltransferase • phospholipase A_2 • apolipoprotein A-I

Lecithin:cholesterol acyltransferase (LCAT) is a glycoprotein with an apparent molecular mass of 67 kDa that consists of 416 residues (1) and 25% of the LCAT mass is carbohydrate. The enzyme is expressed in the liver and secreted into the plasma compartment where it accounts for the synthesis of most of the plasma cholesteryl esters, and thereby contributes to lipid metabolism (2). This enzyme has both a phospholipase A_2 and an acyltransferase activity on lipoproteins, as it catalyzes the transacylation of the *sn*-2 fatty acid of lecithin to the free 3-β hydroxyl group of cholesterol whereby lysolecithin and cholesteryl esters are formed (3). Moreover the enzyme has an esterase activity on monomeric substrates.

Lecithin:cholesterol acyltransferase is active both on low density (LDL) and high density (HDL) lipoproteins, and is primarily associated with HDL particles containing the major activator for LCAT, apolipoprotein A-I (apoA-I) (3). Direct interaction between LCAT and the co-factor apoA-I could not be demonstrated yet (3). Using structural homology calculations based upon threading methods, we proposed that LCAT, like lipases, belongs to the α/β hydrolase fold family (4). We built a 3D model for LCAT using human pancreatic and *Candida antarctica* lipases as templates. This model consists of a central β-sheet made of seven conserved β-strands, connected by four α-helices and separated by loops. A long excursion at residues 211–332 separates the N- and C-terminal regions of LCAT. Using site-directed mutagenesis, we showed that, besides the S181 residue (5), the catalytic triad of LCAT

Abbreviations: CE, cholesteryl ester; DPPC, dipalmitoylphosphatidylcholine; FA, fatty acid; FED, fish-eye disease; FLD, familial LCAT deficiency; HDL, high density lipoprotein; LCAT, lecithin:cholesterol acyltransferase; LDL, low density lipoprotein; PLPC, 1-palmitoyl-2-linoleoylphosphatidylcholine; rHDL, reconstituted HDL particles; WT, wild-type.

[1] To whom correspondence should be addressed.

includes D345 (4), H377 (4, 6), and the oxyanion hole residues F103 and L182 (4). An interfacial recognition domain was proposed between Cys50–Cys74 of LCAT (7, 8) and conserved salt bridges between lipases and LCAT were found essential for enzymatic stability and optimal activity (F. Peelman, B. Vanloo, J. L. Verschelde, C. Labeur, J. Taveirne, A. Verhee, N. Duverger, J. Vanderckhove, J. Tavernier, and M. Rosseneu, unpublished results.).

Several mutations in the LCAT gene lead to impaired enzymatic activity, as recently reviewed by Kuivenhoven et al (9). Mutations causing familial LCAT deficiency (FLD) result in loss of activity on both lipoprotein substrates, while mutations causing fish-eye disease (FED) are associated with partial loss of activity. Among the FED mutations, Kuivenhoven et al., (9) further differentiated between the biochemical phenotype of class 3 mutants, affecting primarily HDL activity and partially LDL activity, and that of class 4 mutants with a selective loss of HDL activity only. FED was first reported by Carlson (10) in two families of Swedish origin. The HDL cholesteryl esters were severely decreased in these patients, while the cholesterol esterification rate was nearly normal. These data suggested that the biochemical profile of FED patients is due to impaired LCAT acyltransferase α-activity on HDL, and normal acyltransferase β-activity on LDL (9, 11). The esterase, phospholipase A_2 and acyltransferase activities of LCAT were characterized using different substrates; esterase activity was measured on monomeric substrates, using phospholipid analogues (12), phospholipase A_2 activity was measured on vesicles (13, 14) and on reconstituted discoidal phospholipid–apoprotein complexes (14). Acyltransferase activity was measured both on vesicles (13, 14), on discoidal and spherical HDL (14–18) and on LDL (3, 7). There is, however, only limited information regarding the relative phospholipase A_2 and acyltransferase activities of wild-type human LCAT and of the mutants causing fish-eye disease. FED mutations were characterized by decreased acyltransferase activity of LCAT on reconstituted HDL compared to LDL (9); however, the phospholipase A_2 activity of the mutants on HDL has not been documented. It is unclear how the two enzymatic activities are related and which residues, besides the catalytic triad, are critical for either activity or for both. The conformation of three of the natural FED mutants was examined in the 3D structure proposed for LCAT (19), showing that residues T123 and N131 belong to the amphipathic helix α 3–4, while N391 is part of the C-terminal helix α His. In the 3D model, the FED mutants T123I, N131D, N391S lie at about 12 Å of each other on the outer surface of the protein, thus creating a putative interface for enzyme–co-factor interactions (19).

In order to further differentiate between the effect of natural FED mutants, we measured their esterase, phospholipase A_2 and acyltransferase activity on several substrates. We further designed and expressed other mutations at the position of the natural FED mutants and at neighbor residues on the hydrophilic side of the amphipathic helices. Based upon the 3D model proposed for human LCAT, we identified a new mutant with the biochemical phenotype of a class 4 FED mutant. These results provide evidence that both phospholipase A_2 and acyltransferase activity on HDL are affected by the natural FED mutations. Comparison of the effects of natural and engineered mutants further delineates a region of LCAT involved in a specific interaction with HDL.

MATERIALS AND METHODS.

Materials

Synthetic 1-palmitoyl-2-linoleoylphosphatidylcholine (PLPC), dipalmitoylphosphatidylcholine (DPPC), 1-pyrenebutyric acid, 1-pyrenehexanoic acid, and cholesterol were obtained from Sigma. Cholesteryl 1-pyrenebutyrate and cholesteryl 1-pyrenehexanoate were purchased from Molecular Probes. [^{3}H]cholesterol was purchased from Amersham whereas [^{3}H]-DPPC was obtained from NEN™ Life Science Product. 1,2-Bis-(1-pyrenebutanoyl)-*sn*-glycero-3-phosphocholine was synthesized from *sn*-glycero-3-phosphocholine and 1-pyrenebutyric acid (Sigma) according to the method of Hendrickson and Rauk (20). The compound was purified by chromatography on a Silica gel Merck 7734 column, equilibrated in CH_2Cl_2, and eluted with a gradient of methanol and water. The bis-pyrenebutanoylphosphatidylcholine eluted at 30% methanol and 3% H_2O. The yield of the synthesis was 26% for the phosphatidylcholine and 13% for the *sn*-1-pyrenebutanoyl-*sn*-2-lyso-PC, which was also obtained during the synthesis. The purity of the product was checked by mass spectrometry and by HPLC on a reverse-phase C18 column, from which it eluted as a single peak.

Molecular modelling

The working model for human LCAT was built using the HOMOLOGY software (Molecular Simulations, San Diego, CA). The pancreatic lipase coordinates were found at the PDB databank entry 1lpb.pdb (21). The distances between residues were measured using the INSIGHT Biosym software.

Site-directed mutagenesis

Mutagenesis was carried out in the pXL 3105 plasmid vector (22), using the Quick Change Site-Directed Mutagenesis method (Stratagene, France). Mutations were built in by PCR using PfU DNA polymerase. After DpnI digestion of the parental dam-methylated template, the synthesized mutated DNA was transformed into *E. coli* XL1-Blue supercompetent cells. Colonies were screened by restriction analysis and mutants were sequenced on an ALF automated sequencer (Pharmacia Biotech). Transient expression of the LCAT cDNA in Cos-1 cells was carried out by lipofectamine (Gibco) transfection. After transfection, the cell culture media (Dulbecco's modified Eagle's medium, Life Technologies, Inc) were changed to Optimem after 16 h and harvested after 48 h. Control experiments without the LCAT plasmid were carried out for each transfection.

The mass of transfected wild-type (WT) and mutant LCAT was assayed by solid-phase enzyme immunoassay using chicken antibodies specific to LCAT, and purified recombinant human LCAT as a standard (4).

Substrate preparation for activity measurements of LCAT

Substrates for esterase activity measurements. A monomeric substrate, consisting of 1,2-bis-(1-pyrenebutanoyl)-*sn*-glycero-3-phosphocholine (bis-pyrene-PC), was used for esterase activity measurement by fluorescence and by HPLC. Bis-pyrene-PC was dissolved in methanol (Biosolve LTD) and stored at −20°C. The concentration of the stock solution was determined by absor-

bance measurement at 342 nm, using a molar absorption coefficient of 75000 $cm^{-1}M^{-1}$.

Reconstituted HDL (rHDL) consisting of dipalmitoylphosphatidylcholine and apoA-I at a molar ratio of 100:1 were prepared by the cholate dialysis method (23), and labeled with [^{3}H]DPPC. The lipid and apolipoprotein composition of the complexes were obtained by an enzymatic colorimetric assay for phospholipid (Biomerieux, France) and by protein quantification of apoA-I by phenylalanine assay by HPLC (24).

Substrates for acyltransferase activity measurements. For measurement of the acyltransferase activity by HPLC, rHDL prepared by cholate dialysis (23) consisted of 1-palmitoyl-2-linoleoyl-phosphatidylcholine–cholesterol–apoA-I at a molar ratio of 100:10:1 (4). The homogeneity and yield of the reconstituted HDL were tested by separation on a Superose 6PG column equilibrated in a 10 mm Tris-HCl buffer, pH 8.0, containing 150 mm NaCl.

For the measurement of the acyltransferase activity on LDL, the lipoproteins were isolated from plasma by sequential ultracentrifugation at densities between 1.007 and 1.063 g/ml and dialyzed against a 10 mm Tris-HCl buffer, pH 8.0, 0.15 m NaCl, 3 mm EDTA, 1 mm NaN_3. LDL was heat inactivated at 56°C and radiolabeled with [^{3}H]cholesterol (7).

Measurement of the esterase and phospholipase A_2 activity of LCAT

Monomeric substrate. The esterase activity of LCAT was measured on monomeric 1,2-bis-(1-pyrenebutanoyl)-*sn*-glycero-3-phosphocholine (15) at a concentration of 0.23 μm. The increase in pyrene monomer fluorescence of the hydrolysis product 1-pyrenebutyric acid was monitored, during 5 min at 398 nm in the cells thermostated at 37°C, by a computer-controlled Aminco Bowman 2 spectrofluorometer. The excitation wavelength was set at 332 nm and the excitation and emission slit widths were 2 and 5 nm, respectively. Data were recorded every 20 sec and the linear portion of the curve between 0 and 2 min was used to calculate the initial reaction velocity Vo.

For quantitative measurement of the esterase activity, the amount of 1-pyrenebutyric acid was measured by HPLC (7). The assay mixture contained 2–4 μm 1,2-bis-(1-pyrenebutanoyl)-*sn*-glycero-3-phosphocholine, 4 mm beta-mercaptoethanol, 4 mg/ml BSA, to which 350 μl cell culture medium and 10 mm Tris-HCL buffer, pH 8.0, 0.15 m NaCl, 3 mm EDTA, 1 mm NaN_3 were added to a final volume of 0.5 ml. The mixture was incubated at 37°C for 10 min and the reaction was stopped by addition of 4 ml chloroform–methanol 2:1 (v/v) containing 1-pyrenehexanoic acid as internal standard. 1-Pyrenebutyric acid was quantified by isocratic HPLC (Waters 600E) on a reverse-phase ODS C18 column (Merck Licrocart 2504), eluted with acetonitrile–water–trifluoroacetic acid 70:30:0.1 (v/v/v). The detection limit of this compound, determined by absorbance measurement on a Waters 486 UV detector set at 342 nm, was around 10 picomole (7). The initial velocity of the enzymatic reaction was determined in the linear portion of the curve, i.e., between 0–10% hydrolysis for bis-pyrene PC.

Reconstituted HDL (rHDL). Phospholipase A_2 activity of LCAT was measured on rHDL labeled with [^{3}H]DPPC. Culture medium (350 μl) was added to a mixture containing labeled rHDL (160 μm DPPC), 4 mm beta-mercaptoethanol, 4 mg/ml BSA, 0.15 m NaCl, 3 mm EDTA, 1 mm NaN_3 in 10 mm Tris-HCL buffer, pH 8.0, and incubated at 37°C for 40 min. The reaction was stopped by addition of 1.9 ml chloroform–methanol 1:2 (v/v), and the mixture was extracted according to Parks, Gebre, and Furbee (25). Free fatty acids and phospholipids were separated by thin-layer chromatography on silica gel plates developed in hexane–diethylether–acetic acid 90:20:1 (v/v/v) and quantified by liquid scintillation counting. The initial velocity was determined in the linear portion of the reaction curves, between 0 and 25% radioactive palmitic acid formation.

Measurement of the acyltransferase activity of LCAT

Reconstituted HDL (rHDL). Cholesterol esterification was monitored by measuring the percentage of cholesteryl esters, by HPLC (26). As previously described (27), the linear portion of the reaction curve enabled calculation of the initial velocity, up to 30% cholesteryl esters formation at apoA-I concentrations around 1 μM to which 500 μl cell medium was added and the reaction proceeded for up to 60 min at 37°C.

Low density lipoproteins (LDL). For acyltransferase activity measurements on LDL, the reaction was initiated by adding 350 μl of the cell culture media to a mixture containing [^{3}H]cholesterol-labeled LDL (20 μm free cholesterol), 4 mm beta-mercaptoethanol, 4 mg/ml BSA, in 10 mm Tris-HCL buffer, pH 8.0, 0.15 m NaCl, 3 mm EDTA, 1 mm NaN_3. The enzymatic reaction was stopped after 3 h by addition of 4 ml hexane–isopropanol 3:2 (v/v). Unesterified cholesterol and cholesteryl esters were separated by thin-layer chromatography on silica gel plates developed in hexane–diethylether–acetic acid 90:20:1 (v/v/v) and quantified by liquid scintillation counting. The linear portion of the reaction corresponded to percentages of cholesterol esterification between 0–5% at a LDL free cholesterol concentration of 20 μm.

RESULTS

Esterase, phospholipase A_2, and acyltransferase activities of natural fish-eye disease mutants

The expression level of WT LCAT in Cos-1 cells was around 2 μg/ml medium, while the natural FED mutants, T123I, N131D, and N391S, were expressed at 60–90% of the wild-type enzyme (**Table 1**). Esterase activity was measured on a monomeric pyrene–PC analogue, both by fluorescence intensity measurements and by HPLC, and phospholipase A_2 activity was measured on a reconstituted rHDL substrate labeled with [^{3}H]DPPC. The acyltransferase activity on rHDL was quantified by HPLC, and that on [^{3}H]cholesterol-labeled LDL was quantified by radioactivity measurement. Control experiments consisting of a mock transfection showed that neither LCAT mass nor acyltransferase activity on rHDL and LDL nor esterase activity on the monomeric substrate were detectable in the cell media. However, the phospholipase A_2 activity on [^{3}H]DPPC-labeled rHDL for the control media was 1.64 ± 0.25 nmol FA/ml medium/h as compared to 8.2 ± 1.7 nmol FA/ml medium/h for the media of WT LCAT transfected COS-1 cells. The phospholipase A_2 activities were corrected for this blank value.

The position of residues 123, 131, and 391 in helices α 3–4 and α His of LCAT is illustrated in an Edmundson-wheel representation in **Fig. 1**. Residue T123 is in the middle of the hydrophilic side of helix α 3–4, while residues N131 and N391 are at the interface between the hydrophobic and hydrophilic sides of helix α 3–4 and α His, respectively.

Table 1 summarizes the specific esterase, phospholipase A_2 and acyltransferase activities of the mutants, expressed as nmol FA/μgLCAT/h and nmol CE/μgLCAT/h, respectively. Esterase activity measured by fluorescence is ex-

TABLE 1. Engineered analogues of the natural FED mutants: mass and specific activities in cell media of mutant transfectants (n = 3)

Mutant	Mass	Esterase Activity Monomeric bis-pyrene PC		PLA_2 Activity rHDL	Acyltransferase Activity	
		Fluorescence	HPLC	^{3}H-DPPC	rHDL HPLC	LDL ^{3}H-cholesterol
	μg/ml	*% WT*	*nmol FA/μg/h*	*nmol FA/μg/h*	*nmol CE/μg/h*	
Wild-type	2.1 ± 0.5	100	0.57 ± 0.1	4.0 ± 1.2	7.0 ± 1.4	0.5 ± 0.1
T123I[a]	1.2 ± 0.3	135 ± 18	0.88 ± 0.20	0.53 ± 0.30	0.01 ± 0.01	0.43 ± 0.08
T123A	1.7 ± 0.3	137 ± 16	0.58 ± 0.15	0.53 ± 0.30	0.01 ± 0.01	0.42 ± 0.08
T123N	1.8 ± 0.4	150 ± 20	0.66 ± 0.15	0.66 ± 0.40	0.01 ± 0.01	0.24 ± 0.07
T123S	1.5 ± 0.1	127 ± 15	0.48 ± 0.10	2.6 ± 0.8	3.3 ± 0.5	0.5 ± 0.1
N131D[a]	2.0 ± 0.4	18 ± 6	0.15 ± 0.05	0.48 ± 0.30	0.04 ± 0.01	0.19 ± 0.05
N131A	1.8 ± 0.5	27 ± 8	0.29 ± 0.05	2.5 ± 0.9	6.0 ± 0.7	0.26 ± 0.1
N391S[a]	2.2 ± 0.3	41 ± 10	0.31 ± 0.08	1.4 ± 0.6	2.5 ± 0.5	0.6 ± 0.1
N391A	1.9 ± 0.2	16 ± 6	0.17 ± 0.08	0.92 ± 0.5	0.77 ± 0.1	0.12 ± 0.05
N391I	1.8 ± 0.5	82 ± 12	0.37 ± 0.10	0.79 ± 0.5	1.40 ± 0.1	0.40 ± 0.08
F382A	1.7 ± 0.4	50 ± 10	0.53 ± 0.10	1.1 ± 0.2	0.01 ± 0.01	0.34 ± 0.1

Esterase activity was measured on monomeric bis-pyrene-PC and phospholipase A_2 (PLA_2) activity was measured on a ^{3}H-labeled DPPC/apoA-I discoidal complex. Acyltransferase activity was measured on rHDL consisting of PLPC/chol/apoA-I and LDL substrates. LCAT, lecithin:cholesterol acyltransferase; bis-pyrene-PC, 1,2-bis-(1-pyrene-butanoyl)-*sn*-glycero-3-phosphocholine; ^{3}H-DPPC-rHDL, consisting of dipalmitoylphosphatidylcholine/apoA-I complex at a molar ratio of 100/1; rHDL, consisting of 1-palmitoyl-2-linoleoylphosphatidylcholine/cholesterol/apoA-I complex at a molar ratio of 100/10/1; LDL, low density lipoprotein.

[a] Natural fish-eye disease (FED) mutants.

pressed as percentage of WT LCAT activity. The T123I mutant was characterized by a specific loss of acyltransferase activity on rHDL, which amounted to around 2% of WT LCAT. In contrast, this mutant retained 86% acyltransferase activity on LDL. The decreased acyltransferase activity of this mutant on rHDL is a consequence of the decreased phospholipase A_2 activity on the same substrate, which amounts to 12% that of WT LCAT, whereas the esterase activity increased by 35–70%, compared to WT LCAT. These specific activities were recalculated as percent of WT LCAT and are depicted in **Fig. 2**, showing increased esterase activity on the monomeric substrate, decreased phospholipase A_2 and acyltransferase activity on rHDL and comparable acyltransferase activity on LDL.

The acyltransferase activity of the N131D mutant on rHDL amounted only to 5% of WT LCAT, while the acyltransferase activity on LDL was decreased by 63% compared to the WT enzyme, a decrease more pronounced than for the T123I mutant. The decrease of phospholipase A_2 activity of the N131D mutant on rHDL paralleled that of acyltransferase activity on the same substrate, while the 82% decrease of esterase activity on a monomeric sub-

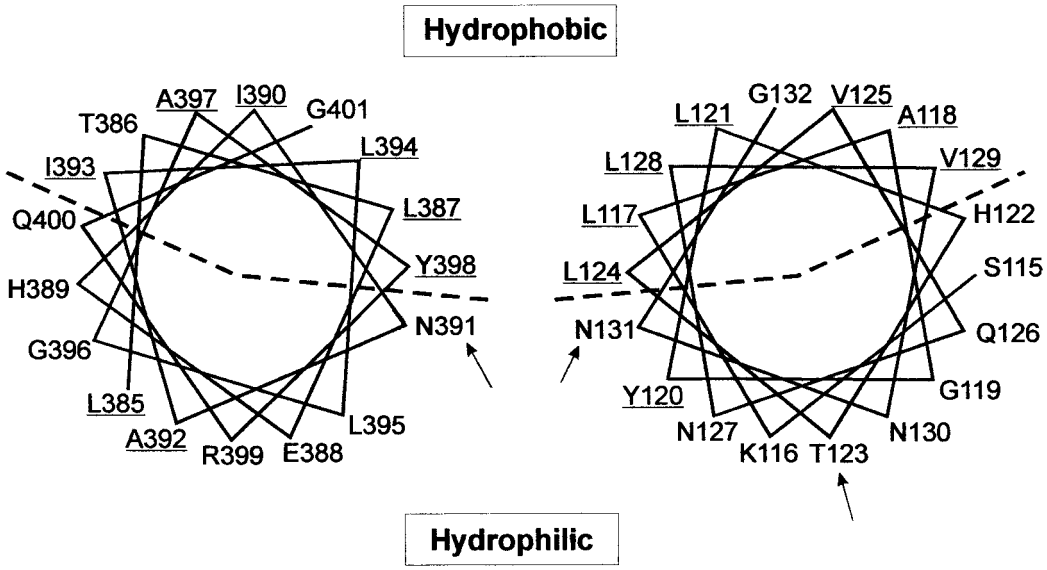

Fig. 1. Edmundson wheel representation of helix α 3–4 (right) and helix α His (left) of LCAT. Hydrophobic residues are underlined and the position of the natural fish eye disease (FED) mutants is indicated by an arrow.

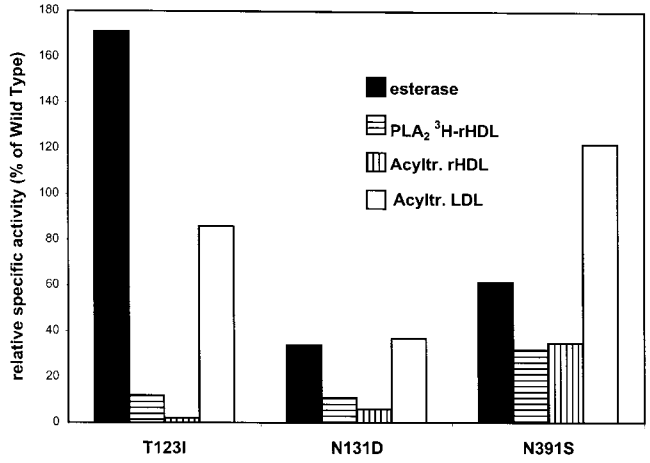

Fig. 2. Mean specific activities, expressed as percent of wild-type LCAT (n = 3), of natural FED mutants, T123I, N131D, and N391S. Esterase activity was measured on monomeric 1,2-bis-(1-pyrenebutanoyl)-*sn*-glycero-3-phosphocholine (esterase); phospholipase A_2 activity on ^{3}H-labeled DPPC/apoA-I discoidal complex (PLA_2 rHDL); acyltransferase activity was measured on PLPC/chol/apoA-I discoidal complex (Acyltr. rHDL); on ^{3}H-cholesterol labeled LDL.

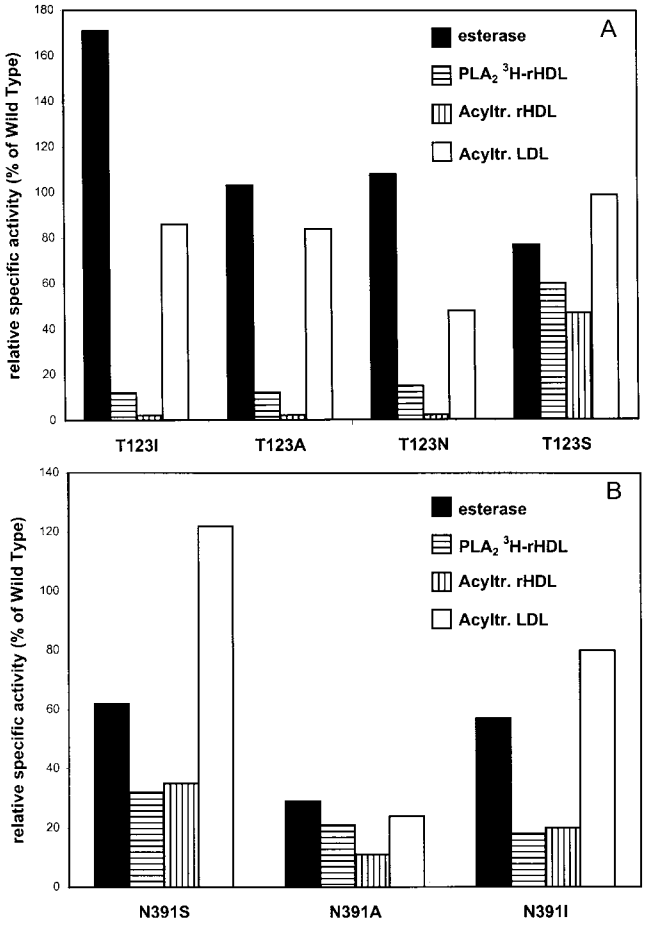

Fig. 3. Mean specific activities, expressed as percent of wild-type LCAT of FED mutant analogues (n = 3) A: at position 123: T123I, T123A, T123N, T123S; B: at position 391: N391S, N391A, N391I. Activity measurements are as described in Fig. 2.

strate was comparable to that of acyltransferase activity measured on LDL (Table 1). This is illustrated in Fig. 2, as mean percent activity relative to WT LCAT, showing that besides a preferential decrease of the activity on rHDL, the natural mutant N131D loses part of its activity on all substrates. The N391S natural FED mutant was characterized by a selective loss of acyltransferase activity on rHDL of 65% relative to WT LCAT, compared to a 20% increase of activity on LDL. A parallel decrease was observed for the phospholipase A_2 activity of this mutant on rHDL, while the esterase activity on a monomeric substrate decreased by 40–60%, compared to WT LCAT (Fig. 2).

Enzymatic activity of analogues of the natural FED mutants

In order to confirm the differences observed between the esterase and acyltransferase activities of natural mutants at positions 123, 131, and 391 of LCAT, we mutated these residues to an alanine (Table 1). T123 was mutated to N and S residues, more hydrophilic than the natural T123I mutant. A N391I variant, more hydrophobic than the natural N391S mutant, was also constructed and expressed in Cos-1 cells. The expression levels of these mutants amounted to 70–90% of WT LCAT, and their specific activity was measured on the substrates listed above (Table 1). As described above for the natural T123I mutant, the T123A, T123N, T123S mutants also induced a class 4 biochemical phenotype, characterized by preferential loss of acyltransferase activity on rHDL, compared to LDL. The decrease of the phospholipase A_2 activity of the mutants on rHDL was comparable to that of the acyltransferase activity. In contrast, the esterase activity was comparable or even slightly higher than that of WT LCAT, as shown by the percentage activity, expressed relative to WT LCAT (**Fig. 3A**). However, these effects varied with the mutations at residue 123. The most conservative T123S substitution retained full acyltransferase activity on LDL and esterase activity on a monomeric substrate, and had 40–50% decrease in phospholipase A_2 and acyltransferase activity on rHDL. The T123N substitution decreased the phospholipase A_2 and acyltransferase activity on rHDL by more than 85%, compared to a 52% decrease of the acyltransferase activity on LDL and an increase of the esterase activity on a monomeric substrate. The effects of the T123I and T123A mutations were comparable, as they both impaired phospholipase A_2 and acyltransferase activity on HDL and preserved acyltransferase activity LDL. The esterase activity of the less hydrophobic T123A mutant on a monomeric substrate increased less than that of the T123I mutant (Fig. 3A). The phospholipase A_2 and acyltransferase activity decrease on rHDL caused by the N131A mutation was less severe than for the natural N131D mutation. The acyltransferase activity of the two mutants on LDL was comparable. Relative to WT LCAT, the acyltransferase activity of the N131A and N131D mutants on rHDL decreased by 15 and 5%, respectively. Both mutations decreased the esterase activity of LCAT on a monomeric substrate by about 70%.

The effect of the N391A and N391I mutations on the different enzymatic activities differed from the natural N391S mutation. The N391A mutant lost 75% acyltransferase activity on LDL and about 90% on rHDL. The relative decrease of the esterase and phospholipase A_2 activities was comparable to that of the acyltransferase activity on LDL, when expressed as absolute activity (Table 1) or as percentage activity relative to WT LCAT (Fig. 3B). Mutation of residue N391 to an isoleucine resulted in a class 4 biochemical phenotype, as the acyltransferase activity on LDL decreased by only 20%, compared to 80% on rHDL. The phospholipase A_2 activity on rHDL decreased by 80% compared to a 20–40% decrease of the esterase activity (Fig. 3B).

Esterase, phospholipase A_2 and acyltransferase activity of engineered mutants in the vicinity of the natural FED mutants

As described above, the natural FED mutants T123I and N131D both belong to the amphipathic helix α 3–4, spanning residues 116–134, while N391 belongs to the parallel C-terminal helix α His (19). We mutated other residues, located in the vicinity of T123 and N131, in order to investigate their contribution to the enzymatic activity. Residues Q126, N127, and N130 of the hydrophilic face of helix α 3–4 were mutated to an alanine, to decrease the polar character of this helical segment and prevent putative hydrogen bond formation by these residues. N130 was mutated to an aspartic acid to introduce a negative charge at that position, in analogy with the natural N131D mutation. All mutants were expressed at significant levels and their specific activity was measured on all substrates. The results, summarized as absolute activity in **Table 2** and depicted as percentage activity in **Fig. 4A**, show that all mutants lost 20–60% acyltransferase activity on rHDL and LDL and esterase activity on a monomeric substrate. None of these mutations induced a biochemical phenotype similar to that of either FED or FLD mutants. Residue Y120, located at the interface between hydrophobic and hydrophilic faces, N-terminal of helix α 3–4 (**Fig. 5**), was also mutated to an alanine. In contrast to previous mutants, the Y120A mutant lost both esterase and acyltransferase activity (Table 2, Fig. 4A). As residue N391 is located on the hydrophilic face of helix α His, additional mutations to an alanine were carried out at residues E388 and H389, both on the hydrophilic face of this helix. The E388A mutant retained esterase activity, and its acyltransferase activity was even increased on rHDL and LDL. The activity of the H389A mutant was retained on rHDL, whereas it decreased by 60% on LDL and by 30% on the monomeric substrate (Table 2, Fig. 4B). Finally, we mutated residue F382 to an alanine, as this residue which lies N-terminal of helix α His is in close vicinity to the catalytic triad in the 3D model of LCAT (Fig. 5). The results listed in Table 1 and depicted in Fig. 4B, demonstrate that this mutant induces a class 4 FED biochemical phenotype, with a specific decrease of phospholipase A_2 and acyltransferase ac-

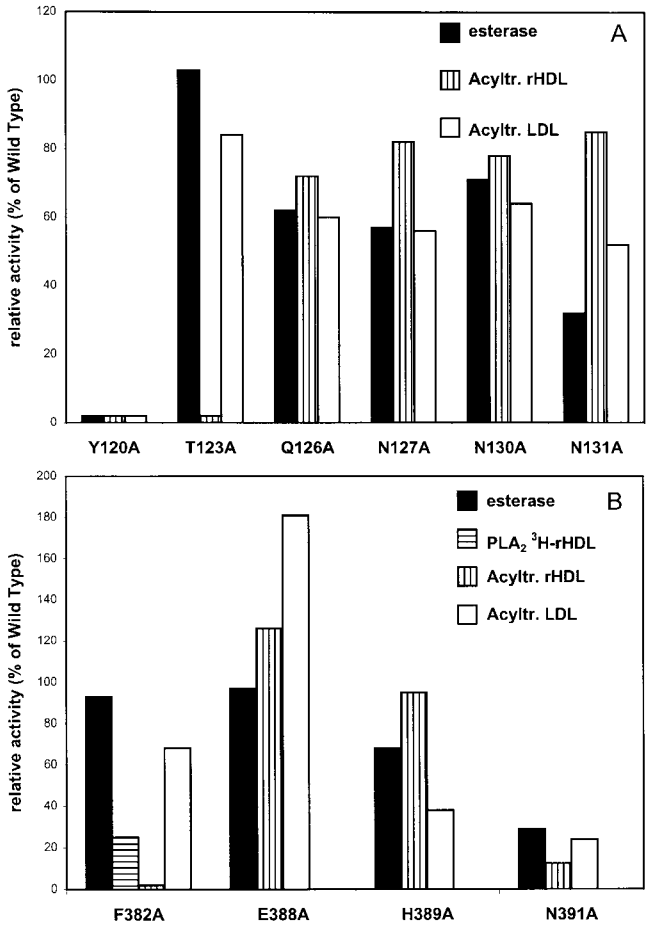

Fig. 4. Mean specific activities, expressed as percent of wild-type LCAT, of expressed LCAT mutants (n=3). A: mutations in helix α 3–4: Y120A, T123A, Q126A, N127A, N130A, N131A; B: in helix α His: F382A, E388A, H389A, N391A. Measurements are as described in Fig. 2.

TABLE 2. Engineered mutants in the vicinity of the natural FED mutants: mass and specific activities in cell media of mutant transfectants (n = 3)

Mutant	Mass	Esterase Activity Monomeric Bis-pyrene PC HPLC	Acyltransferase Activity rHDL HPLC	Acyltransferase Activity LDL [^{3}H]cholesterol
	μg/ml	*nmol FA/μg/h*	*nmol CE/μg/h*	
Wild-type	2.1 ± 0.5	0.57 ± 0.1	7.0 ± 1.4	0.5 ± 0.05
Y120A	1.0 ± 0.4	0.01 ± 0.01	0.01 ± 0.02	0.01 ± 0.02
Q126A	1.7 ± 0.3	0.35 ± 0.08	5.0 ± 1.1	0.30 ± 0.07
N127A	1.9 ± 0.3	0.32 ± 0.10	5.7 ± 1.2	0.28 ± 0.06
N130A	1.8 ± 0.4	0.40 ± 0.12	5.5 ± 1.1	0.32 ± 0.08
N130D	1.8 ± 0.3	0.66 ± 0.15	3.0 ± 0.8	0.78 ± 0.10
E388A	1.6 ± 0.4	0.55 ± 0.10	8.8 ± 1.2	0.91 ± 0.15
H389A	1.5 ± 0.5	0.39 ± 0.08	6.7 ± 0.9	0.19 ± 0.03
F382A	1.7 ± 0.5	0.53 ± 0.12	0.01 ± 0.02	0.34 ± 0.05

Esterase activity was measured on monomeric bis-pyrene-PC. Acyltransferase activity was measured on rHDL consisting of PLPC/cholesterol/apoA-I and LDL substrates. LCAT, lecithin:cholesterol acyltransferase; bis-pyrene-PC, 1,2-bis-(1-pyrene-butanoyl)-*sn*-glycerol-3-phospho-choline; rHDL, consisting of 1-palmitoyl-2-linoleoyl-phosphatidylcholine/cholesterol/apoA-I at a molar ratio of 100/10/1; LDL, low density lipoproteins.

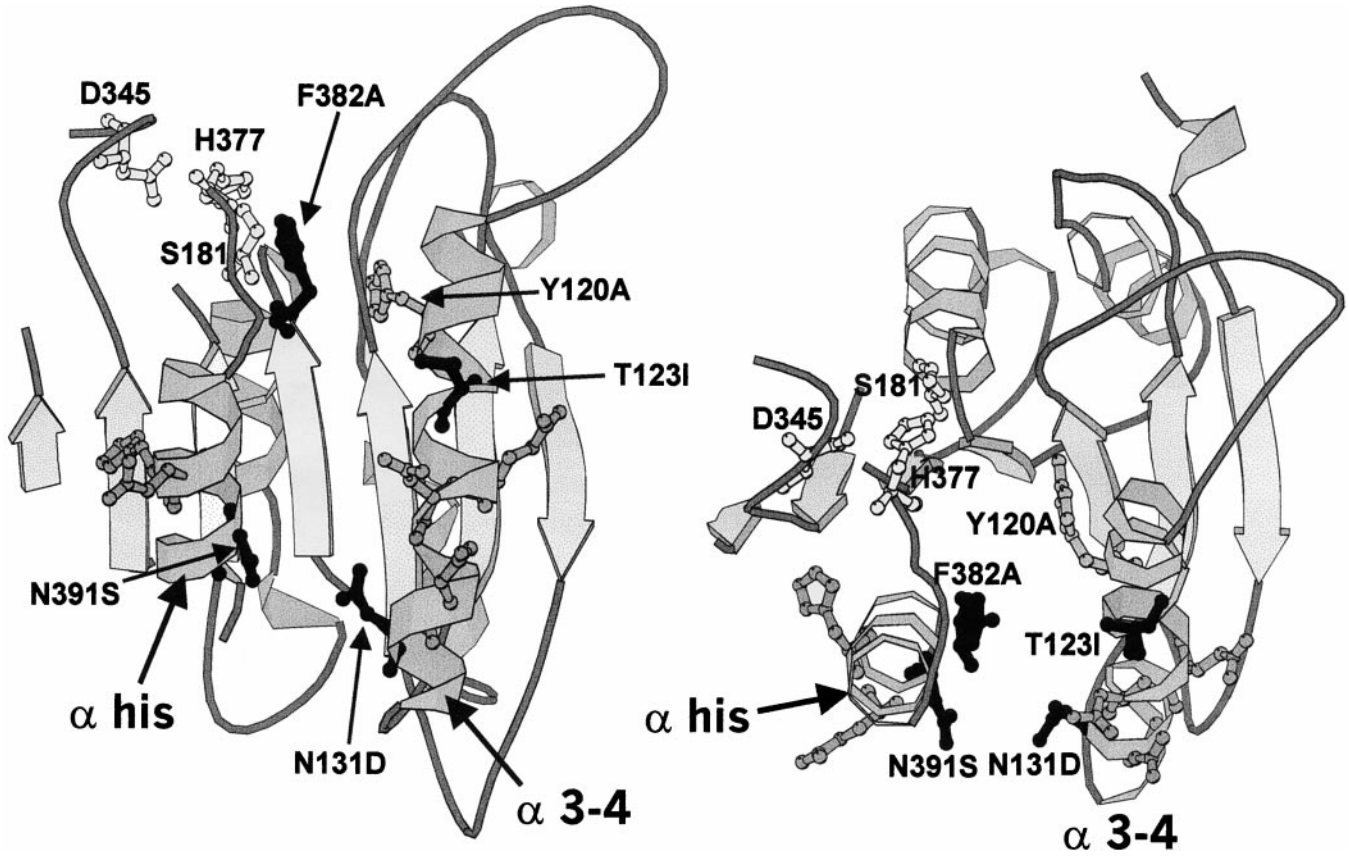

Fig. 5. Position of the natural and engineered FED mutants in the working model proposed for the LCAT structure. Left: front view of helix α 3–4 and α His and of the central β-sheet; right: top view of the same model. Catalytic triad residues S181, D345 and H377 are indicated. Natural mutants T123A, N131D, N391S and the engineered mutant F382A are colored in black. Engineered mutants at residues Y120, Q126, N127, N130, E388, and H389 are colored in white.

tivity on rHDL, combined with normal esterase activity on a monomeric substrate and normal acyltransferase activity on LDL.

DISCUSSION

In this paper we measured separately the esterase activity on a monomeric substrate, phospholipase A_2 activity on rHDL, and acyltransferase activity on rHDL and LDL of wild-type LCAT and of natural FED mutants and analogues. We show that impaired phospholipase A_2 activity accounts for decreased acyltransferase activity on rHDL and that FED mutations specifically affect phospholipase A2 activity on HDL, whereas esterase activity on the monomeric substrate and acyltransferase activity on LDL are retained. This is in contrast with the classic FLD mutations that impair activity on all substrates (3–6, 9).

While the preferential decrease of the acyltransferase activity of FED mutants on rHDL, compared to LDL, has been well documented, the effect of these mutations on phospholipase A_2 activity had not been studied in detail. Only Holmquist and Carlson (28) reported a decreased phospholipase A_2 activity in the plasma of a FED patient. As FED LCAT mutants have normal esterase activity, these mutations do not directly affect the catalytic triad (29, 30). We used both a monomeric fluorescent phospholipid analogue, as proposed by Bonelli and Jonas (12), and discoidal rHDL labeled with [^{3}H]DPPC (25) to assay the esterase and phospholipase A_2 activity of the FED mutants. These mutants have normal or even increased activity on the monomeric substrate, whereas the phospholipase A_2 activity on rHDL was decreased, as reported by Holmquist and Carlson (28), on the plasma of a FED patient. When the phospholipase A_2 activity of wild-type LCAT was measured on rHDL containing 5 mole % cholesterol, we found that it amounted to around 10% of the total (phospholipase A_2 + acyltransferase) enzymatic activity (data not shown), in agreement with previous reports (31). During the chemical reaction catalyzed by LCAT, a fatty acid is cleaved at the *sn*-2 position of phosphatidylcholine and transferred to the free hydroxyl group of cholesterol. Our findings suggest that the decreased LCAT activity on HDL in FED is a consequence of a decreased phospholipase A_2 activity and not of an impaired transfer of the fatty acid to cholesterol.

Kuivenhoven et al. (9) divided the different molecular defects in LCAT into four classes. Class 4 consists of mutations, such as T123I, with a typical FED phenotype, i.e., with normal acyltransferase activity on LDL, together with severely reduced activity on HDL. Class 3 FED mutations

such as N131D and N391S have decreased acyltransferase activity on both HDL and LDL. To further differentiate between these two classes, we overexpressed the T123I, N131D, and N391S mutants together with other mutations at these positions. Four different mutations at position 123 (T123I, T123N, T123A, T123S) all induced a class 4 biochemical phenotype (32) with specific decrease of phospholipase A_2 and acyltransferase activity on HDL, together with preserved activity on LDL and on a monomeric substrate, indicating that the mutants are still catalytically active. Residue T123 is in the middle of the hydrophilic face of the amphipathic helix α3–4, and mutations at the position have minimal impact on LCAT structure. This is in agreement with the data of Adimoolam et al. (30), who showed that the T123I LCAT mutant has the same CD spectrum, tryptophan fluorescence emission properties, and identical GuHCl denaturation profile and free energy of denaturation as wild-type LCAT. Phospholipase A_2 and acyltransferase activities of LCAT on HDL seem to strictly require a threonine residue at position 123, as even the highly conservative T123S mutation decreased both activities by 50%.

Class 3 mutations N131D and N391S have decreased acyltransferase activity on both HDL and LDL (9, 33, 34). When overexpressed in Cos-1 cells, the phospholipase A_2 and acyltransferase activities of the mutants on HDL decreased more than the esterase activity on a monomeric substrate or acyltransferase activity on LDL. These natural mutations thus specifically effect HDL activity, although this effect is less pronounced than for the T123I mutation. All mutants expressed at position 123 decreased LCAT activity on HDL, while the activity of the mutants engineered at positions 131 and 391 was dependent upon the mutation. The N131A LCAT mutant had normal activity on HDL and lost the FED biochemical phenotype typical for the N131D mutant. The N131D mutation introduces a negative charge, C-terminal of helix α3–4, which might interfere with the helical dipole and impair helical stability. This suggests that, in contrast to T123, residue N131 is not a prerequisite for full LCAT activity on HDL. The N391A mutation decreased the enzymatic activities on all substrates to less than 30% of wild-type LCAT. The enzymatic activity profile of the N391I mutant resembled that of the natural N391S mutant, as the activity decrease was more pronounced for HDL than for the other substrates. In the 3D model we proposed for human LCAT (4), residues N131 and N391 lie within 5 Å of each other, at the interface between the hydrophilic and hydrophobic sides of the amphipathic helices α 3–4 and α His. Mutations at positions 131 and 391 might either destabilize these helices or perturb their relative orientation.

Because the three FED mutations T123I, N131D, and N391S have decreased activity on HDL, we previously proposed that the parallel helices α 3–4 and α His, which are on the same side of the central β sheet of the LCAT fold, might specifically interact with HDL (19). To test this hypothesis, we mutated residues Q126, N127, and N130 on the hydrophilic face of helix α 3–4 and residues E388 and H389 on the hydrophilic side of helix α His to an alanine and tested the activity of these mutants on different substrates. These mutations did not perturb the recognition of the HDL substrate, as their specific activity on rHDL amounted to 72–126% of the wild-type LCAT activity. This suggests that the interaction between LCAT and HDL does not involve the entire length of these helices, but is restricted to particular residues at the extremity of these helices. Among these mutants, only the N130D mutation preferentially decreased the LCAT activity on rHDL, while the N130A mutation did not. As observed for the natural N131D mutation, a negative charge C-terminal of helix α 3–4 in this mutant might affect the helical dipole and destabilize this helix. The loss of a negative charge through the E388A substitution in helix α His increased the acyltransferase activity on both HDL and LDL, suggesting that negative charges C-terminal of both helices impair LCAT activity. The Y120A mutant, N-terminal of helix α 3–4 lost activity on all substrates, suggesting that this residue might be critical for the folding and stability of the LCAT core. In the model for LCAT, Y120 lies at the interface between the hydrophilic and hydrophobic faces of the amphipathic helix α 3–4, and its interaction with the hydrophobic side of beta-strand 3, especially with residue P101, probably contributes to the stability of the hydrophobic core (Figs. 1, 5). A newly engineered F382A mutant was designed on the basis of its location and orientation in the 3D model proposed for LCAT (4), where it could interact with a molecule of cholesterol when fit into the active site cavity. This residue lies N-terminal of helix α His, in close proximity to the active site cavity, within 7 Å of the class 4 T123I mutant. The results of the phospholipase A_2 and acyltransferase activity measurements suggest that residues T123 and F382 both contribute to the α-activity of LCAT on an HDL substrate. Any substitution of T123, either by a hydrophilic or an hydrophobic residue, decreases both phospholipase A_2 and acyltransferase activity on rHDL. The increased esterase activity of the T123I mutant on a monomeric substrate might be due to an increased hydrophobic interaction with the substrate. Our results thus propose a structural basis for the differentiation between class 3 and class 4 FED mutants. Class 3 mutants are residues specifically involved in the activation of the enzyme by its co-factor apoA-I, i.e., T123 and F382, and they are therefore essential for the α-activity of LCAT on HDL. Class 4 mutants are residues contributing to the recognition of lipoprotein substrates by LCAT, through an optimal conformation of enzyme and substrate. In the classic FLD (Familial LCAT Deficiency) mutants, all enzymatic activities are severely impaired and we have previously shown that FLD mutations either perturb the architecture of the catalytic triad, impair the accessibility to the catalytic residues, or affect the fold of the enzyme (19).

The mechanism of action of LCAT is similar to that of lipases, as these enzymes share a common α–β hydrolase fold (4). In the first step of the enzymatic reaction, a fatty acid is cleaved from either a triglyceride or a phospholipid and forms an acyl intermediate with the active site serine (35). In lipases, this fatty acid is subsequently released through an hydrophilic attack by the hydroxyl

group of a water molecule. In LCAT, this hydroxyl group is provided by a more hydrophobic long-chain alcohol or sterol, to which the fatty acid is transfered (36). Due the lack of a crystallized structure for LCAT, the hydrophobic pockets accommodating the cleaved fatty acid and/or the sterol or alcohol acceptor have not been identified yet. This substrate might have an orientation similar to that of an inhibitor co-crystallized with pancreatic lipase (21). Further analogy between LCAT and lipases, i.e., pancreatic lipase and bile salt-activated lipase, is the co-factor requirement for the activation of these enzymes. In lipases, conformational changes increase the accessibility of the substrate to the active site (21, 37). In pancreatic lipase, the interaction with the substrate and colipase induces conformational changes in the region N-terminal of helix α His. The conformational change of the bile salt-activated lipase upon binding of one bile salt molecule occurs N-terminal of helix α 3–4. In analogy with lipases, the activation of LCAT might occur through similar conformational changes in the corresponding regions of LCAT, N-terminal of α 3–4 and α His, to which both residues T123 and F382 belong.

In summary, these experimental data strongly support the hypothesis previously proposed on the basis of molecular modeling (19), that one layer of helices in the α/β hydrolase fold of LCAT is involved in the lipoprotein substrate recognition, and that the conformation and orientation of these helices are critical for optimal activity. Measurements of LCAT activation by wild-type apoA-I and by natural or engineered mutants (38, 39) suggest that residues 120–160 of apoA-I contribute to the LCAT activation properties of this apolipoprotein, and might represent the corresponding segment of apoA-I interacting with LCAT. (3).

Manuscript received 12 October 1999, in revised form 25 January 2000, and in re-revised form 15 February 2000.

REFERENCES

1. McLean, J., C. Fielding, D. Drayna, H. Dieplinger, B. Baer, W. Kohr, W. Henzel, and R. Lawn. 1986. Cloning and expression of human lecithin-cholesterol acyltransferase cDNA. *Proc. Natl. Acad. Sci. USA.* **83:** 2335–2339.
2. Glomset, J. A. 1968. The plasma lecithin:cholesterol acyltransferase reaction. *J. Lipid Res.* **9:** 155–167.
3. Jonas, A. 1998. Regulation of lecithin:cholesterol acyltransferase activity. *Prog. Lipid Res.* **37:** 209–234.
4. Peelman, F., N. Vinaimont, A. Verhee, B. Vanloo, J. L. Verschelde, C. Labeur, M. S. Seguret, N. Duverger, G. Hutchinson, J. Vandekerckhove, J. Tavernier, and M. Rosseneu. 1998. A proposed architecture for lecithin cholesterol acyl transferase (LCAT): identification of the catalytic triad and molecular modeling. *Protein Sci.* **7:** 587–599.
5. Francone, O. L., and C. J. Fielding. 1991. Structure-function relationships in human lecithin:cholesterol acyltransferase. Site-directed mutagenesis at serine residues 181 and 216. *Biochemistry.* **30:** 10074–10077.
6. Adimoolam, S., Y. P. Lee, and A. Jonas. 1998. Mutagenesis of highly conserved histidines in lecithin cholesterol acyltransferase: identification of an essential histidine (His 377). *Biochem. Biophys. Res. Commun.* **243:** 337–341.
7. Peelman, F., B. Vanloo, O. Perez-Mendez, A. Decout, J. L. Verschelde, C. Labeur, N. Vinaimont, A. Verhee, N. Duverger, R. Brasseur, J. Vandekerckhove, J. Tavernier, and M. Rosseneu. 1999. Characterization of functional residues in the interfacial recognition domain of lecithin cholesterol acyltransferase (LCAT). *Protein Eng.* **12:** 71–78.
8. Adimoolam, S., and A. Jonas. 1997. Identification of a domain of lecithin-cholesterol acyltransferase that is involved in interfacial recognition. *Biochem. Biophys. Res. Commun.* **232:** 783–787.
9. Kuivenhoven, J. A., H. Pritchard, J. Hill, J. Frohlich, G. Assmann, and J. Kastelein. 1997. The molecular pathology of lecithin:cholesterol acyltransferase (LCAT) deficiency syndromes. *J. Lipid Res.* **38:** 191–205.
10. Carlson, L. A. 1979. A further case of fish-eye disease. *Lancet.* **2:** 1376–1377.
11. Carlson, L. A., and L. Holmquist. 1985. Evidence for the presence in human plasma of lecithin:cholesterol acyltransferase activity (beta-LCAT) specifically esterifying free cholesterol of combined pre-beta- and beta-lipoproteins. Studies of fish eye disease patients and control subjects. *Acta Med. Scand.* **218:** 197–205.
12. Bonelli, F. S., and A. Jonas. 1992. Continuous fluorescence assay for lecithin:cholesterol acyltransferase using a water-soluble phosphatidylcholine. *J. Lipid Res.* **33:** 1863–1869.
13. Yamazaki, S., T. Mitsunaga, Y. Furukawa, and T. Nishida. 1983. Interaction of lecithin-cholesterol acyltransferase with human plasma lipoproteins and with lecithin-cholesterol vesicles. *J. Biol. Chem.* **258:** 5847–5853.
14. Jonas, A. 1986. Synthetic substrates of lecithin:cholesterol acyltransferase. *J. Lipid Res.* **27:** 689–698.
15. Bonelli, F. S., K. E. Kezdy, and A. Jonas. 1987. A continuous fluorescence assay for lecithin cholesterol acyltransferase. *Anal. Biochem.* **166:** 204–207.
16. Sparks, D. L., and P. H. Pritchard. 1989. The neutral lipid composition and size of recombinant high density lipoproteins regulates lecithin:cholesterol acyltransferase activity. *Biochem. Cell Biol.* **67:** 358–364.
17. Pownall, H. J., Q. Pao, and J. B. Massey. 1985. Acyl chain and headgroup specificity of human plasma lecithin:cholesterol acyltransferase. Separation of matrix and molecular specificities. *J. Biol. Chem.* **260:** 2146–2152.
18. Vanloo, B., J. Morrison, N. Fidge, G. Lorent, L. Lins, R. Brasseur, J. M. Ruysschaert, J. Baert, and M. Rosseneu. 1991. Characterization of the discoidal complexes formed between apoA-I-CNBr fragments and phosphatidylcholine. *J. Lipid Res.* **32:** 1253–1264.
19. Peelman, F., J. L. Verschelde, B. Vanloo, C. Ampe, C. Labeur, J. Tavernier, J. Vandekerckhove, and M. Rosseneu. 1999. Effects of natural mutations in lecithin:cholesterol acyltransferase on the enzyme structure and activity. *J. Lipid Res.* **40:** 59–69.
20. Hendrickson, H. S., and P. N. Rauk. 1981. Continuous fluorometric assay of phospholipase A_2 with pyrene-labeled lecithin as a substrate. *Anal. Biochem.* **116:** 553–558.
21. Egloff, M. P., F. Marguet, G. Buono, R. Verger, C. Cambillau, and H. van Tilbeurgh. 1995. The 2.46 A resolution structure of the pancreatic lipase-colipase complex inhibited by a C11 alkyl phosphonate. *Biochemistry.* **34:** 2751–2762.
22. Seguret, M. S., M. M. Latta, G. Castro, G. Luc, J. C. Fruchart, E. Rubin, P. Denefle, and N. Duverger. 1996. Potential gene therapy for lecithin-cholesterol acyltransferase (LCAT)-deficient and hypoalphalipoproteinemic patients with adenovirus-mediated transfer of human LCAT gene. *Circulation.* **94:** 2177–2184.
23. Matz, C. E., and A. Jonas. 1982. Micellar complexes of human apolipoprotein A-I with phosphatidylcholines and cholesterol prepared from cholate-lipid dispersions. *J. Biol. Chem.* **257:** 4535–4540.
24. Vanloo, B., J. Taveirne, J. Baert, G. Lorent, L. Lins, J. M. Ruyschaert, and M. Rosseneu. 1992. LCAT activation properties of apo A-I CNBr fragments and conversion of discoidal complexes into spherical particles. *Biochim. Biophys. Acta.* **1128:** 258–266.
25. Parks, J. S., A. K. Gebre, and J. W. Furbee. 1999. Lecithin-cholesterol acyltransferase. Assay of cholesterol esterification and phospholipase A_2 activities. *Methods Mol. Biol.* **109:** 123–131.
26. Corijn, J., R. Deleys, C. Labeur, B. Vanloo, L. Lins, R. Brasseur, J. Baert, J. M. Ruysschaert, and M. Rosseneu. 1993. Synthetic model peptides for apolipoproteins. II. Characterization of the discoidal complexes generated between phospholipids and synthetic model peptides for apolipoproteins. *Biochim. Biophys. Acta.* **1170:** 8–16.
27. Matz, C. E., and A. Jonas. 1982. Reaction of human lecithin cholesterol acyltransferase with synthetic micellar complexes of apolipoprotein A-I, phosphatidylcholine, and cholesterol. *J. Biol. Chem.* **257:** 4541–4546.
28. Holmquist, L., and L. A. Carlson. 1987. Alpha-lecithin:cholesterol

acyltransferase deficiency. Lack of both phospholipase A_2 and acyltransferase activities characteristic of high density lipoprotein lecithin:cholesterol acyltransferase in fish eye disease. *Acta Med. Scand.* **222:** 23–26.
29. Klein, H. G., N. Duverger, J. J. Albers, S. Marcovina, H. B. Brewer, Jr., and S. Santamarina-Fojo. 1995. In vitro expression of structural defects in the lecithin-cholesterol acyltransferase gene. *J. Biol. Chem.* **270:** 9443–9447.
30. Adimoolam, S., L. Jin, E. Grabbe, J. J. Shieh, and A. Jonas. 1998. Structural and functional properties of two mutants of lecithin-cholesterol acyltransferase (T123I and N228K). *J. Biol. Chem.* **273:** 32561–32567.
31. Czarnecka, H., and S. Yokoyama. 1993. Regulation of lecithin-cholesterol acyltransferase reaction by acyl acceptors and demonstration of its "idling" reaction. *J. Biol. Chem.* **268:** 19334–19340.
32. Funke, H., A. von Eckardstein, P. H. Pritchard, J. J. Albers, J. J. Kastelein, C. Droste, and G. Assmann. 1991. A molecular defect causing fish eye disease: an amino acid exchange in lecithin-cholesterol acyltransferase (LCAT) leads to the selective loss of alpha-LCAT activity. *Proc. Natl. Acad. Sci. USA.* **88:** 4855–4859.
33. Kuivenhoven, J. A., E. van-Voorst-tot-Voorst, H. Wiebusch, S. M. Marcovina, H. Funke, G. Assmann, P. H. Pritchard, and J. J. Kastelein. 1995. A unique genetic and biochemical presentation of fish-eye disease. *J. Clin. Invest.* **96:** 2783–2791.
34. Hill, J. 1994. The molecular pathology of lecithin:cholesterol acyltransferase deficiency. Ph.D Thesis.
35. Jauhiainen, M., W. Yuan, M. H. Gelb, and P. J. Dolphin. 1989. Human plasma lecithin-cholesterol acyltransferase. Inhibition of the phospholipase A_2-like activity by sn-2-difluoroketone phosphatidylcholine analogues. *J. Biol. Chem.* **264:** 1963–1967.
36. Zhou, G. Y., M. Jauhiainen, K. Stevenson, and P. J. Dolphin. 1991. Human plasma lecithin:cholesterol acyltransferase. Preparation and use of immobilized p-aminophenylarsenoxide as a catalytic site-directed covalent ligand in enzyme purification. *J. Chromatogr.* **568:** 69–83.
37. Wang, X., C. S. Wang, J. Tang, F. Dyda, and X. C. Zhang. 1997. The crystal structure of bovine bile salt activated lipase: insights into the bile salt activation mechanism. *Structure.* **5:** 1209–1218.
38. Dhoest, A., Z. Zhao, B. De Geest, E. Deridder, A. Sillen, Y. Engelborghs, D. Collen, and P. Holvoet. 1997. Role of the Arg123-Tyr166 paired helix of apolipoprotein A-I in lecithin:cholesterol acyltransferase activation. *J. Biol. Chem.* **272:** 15967–15972.
39. Sorci-Thomas, M. G., L. Curtiss, J. S. Parks, M. J. Thomas, M. W. Kearns, and M. Landrum. 1998. The hydrophobic face orientation of apolipoprotein A-I amphipathic helix domain 143-164 regulates lecithin:cholesterol acyltransferase activation. *J. Biol. Chem.* **273:** 11776–11782.